Relativistic quasifree scattering of hadrons

R. J. Peterson[*]

Department of Physics, University of Colorado, Boulder, Colorado 80309-0390, USA

Continuum spectra of hadrons scattered without charge exchange by complex nuclei, under conditions such that incoherent elastic scattering from bound nucleons can be considered as quasifree, have been transformed into relativistic single-nucleon responses, in a fashion familiar for electron spectra. These hadron responses are subjected to tests of their scaling properties, for changes in momentum transfer, nuclear mass, and specific hadron beams. Scaling is indeed found for some beam energies and angles, with more success for light nuclei.

I. INTRODUCTION

Modern analyses of quasifree electron scattering on complex nuclei have been presented as single-nucleon responses with relativistic kinematics [1–4], based upon the conditions for incoherent quasifree scattering found in Ref. [5]. These analyses are designed to cover all nuclei, by including a Fermi momentum which changes with nuclear mass. These internal momenta k_F have been taken from fits to quasifree electron spectra [6], with newer data used to replace the values inferred in Ref. [7]. Here, the corresponding intermediate energy hadron quasifree spectra without charge exchange (NCX) will be presented in the same relativistic response format, for a closer comparison to electron scattering responses and to the large body of theoretical work inspired by the electron data. Reference [8] includes a survey of these methods for ^{12}C at large momentum transfers. Scaling, in which two or more observables are combined into a single variable whose responses agree, is a powerful demonstration that the assumptions made for the responses are indeed valid.

The present work will explore a wide range of momentum transfers for quasifree scattering of elementary hadrons to determine the limits of the methods used, with a very wide range of nuclear masses, from $A = 6$ through $A = 208$. Quasifree scattering of electrons has found only small alterations for the in-medium electromagnetic interactions [9,10], but the strong interaction will influence the in-medium collisions of hadronic beams with bound nucleons, and possibly alter the responses in several ways. The wide range of data considered in the present work will serve to examine these possibilities, in a manner fully consistent with the electron scattering analyses. There are other scaling systems than the one used here, compared to one another for hadrons in Ref. [11].

The relativistic responses for electrons have been found to scale in two fashions. The scaling variable ψ used here is the least momentum of the bound nucleon that may scatter a beam particle to a given energy transfer ω and momentum transfer q (as a fraction of the Fermi momentum k_F) to a single bound nucleon; here, the response will be called $\Phi(\psi)$. Scaling of the first kind is found for responses by a given beam on a given nucleus that are independent of the momentum transfer to the beam, while scaling of the second kind is noted when responses at a given momentum transfer are the same for all nuclear targets of mass A for a given beam and momentum transfer q [12,13]. When both the first and second kinds of scaling are noted, the result has been called Superscaling [2,13–15]. A universal curve has been found to match the electron scattering charge responses f_L to demonstrate Superscaling [4,6]. A third kind of scaling has been defined for hadron quasifree responses when all relevant hadron beams yield the same responses at a given momentum transfer on a given nucleus [16], and this third kind of scaling has been used to connect electroweak scattering of electrons to create nuclear responses for reactions with neutrinos [17].

In addition to the requirements for quasifree scattering, scaling also assumes that the single-nucleon spin and isospin responses of nuclei are the same as for free-space scattering. The wide range of beams (electrons and hadrons), beam energies, and momentum transfers will provide a severe test of this assumption, and perhaps open the door to understanding nuclear response modifications.

Most of the information found in quasifree single-nucleon responses is determined by the internal motion of the bound nucleons, here modeled as a relativistic Fermi gas (RFG) to generate comparison curves [1–4]. This Fermi gas is only a simplification of the true single-particle nuclear response [18] but allows a simple curve to seek more interesting features of these measured responses. A recent comparison of electron quasifree data to model predictions was able to quantify the limits of Fermi gas models [19]. The responses of this work will be compared to the expectations of the RFG for momentum transfers q greater than twice the Fermi momentum k_F. At smaller momentum transfers some of the RFG response will be blocked by the Pauli Principle, since some nuclear momentum states are occupied, banning scattering into those states. This blocking effect for hadron quasifree scattering has recently been examined for hadron integrated cross sections [20].

All of the expressions to be used in this work, defining the scaling variable ψ, the response $\Phi(\psi)$, the RFG, and the Pauli blocking, are to be found in the Appendix.

---

[*]Jerry.Peterson@Colorado.edu

II. THE DATA

Measured inclusive (only one outgoing particle detected) spectra without charge exchange (NCX) for hadrons scattered from ^{6}Li, carbon, calcium, zirconium (or niobium), and lead (and bismuth) will be presented as their relativistic responses $\Phi(\psi)$ for scaling of the first and third kinds. A wider range of nuclear masses has been studied with several hadron beams, and will be used to test scaling of the second kind. The beams used were 500 MeV pions (of both signs) [21,22], 820 MeV π^- [23], 367 MeV K^+ [24], 392, 400, and 420 MeV protons [25–29], 558 MeV protons [30], 795 MeV protons [31], and 1014 MeV protons [32]. Summaries of trends will be made by interpolating these responses at $\psi = 0$ and $\psi = -0.8$, with the $\psi = 0$ data at the expected maximum of the responses, and $\psi = -0.8$ at smaller energy losses less subject to complications of pion production and more subject to collective effects.

Momentum transfers q to the beam particle range from 269 [32] to 819 MeV/c [27], as computed for free elastic scattering from protons at the scattering angles of the experiments. These momentum transfers vary across a spectrum at a fixed scattering angle, but will be cited in this work as the free hadron-proton elastic scattering momentum transfer. The conditions for incoherent quasifree scattering of these beams from one-and-only-one bound nucleon become valid near $q = 400$ MeV/c [5]. All of the beam energies are sufficient to meet these conditions. Only statistical uncertainties as published will be shown; an additional systematic uncertainty near 10% is recognized, but not included in the response data. Most data were taken with magnetic spectrometers, normalized to elastic scattering on free protons in a hydrocarbon sample. The 558 MeV (p, px) data were taken with scintillation counters, with particle identification to exclude deuterons, but worse energy resolution [30]. Using these data, it is concluded that deuteron contamination of the proton spectra analyzed in the present work is very small.

III. SCALING OF THE FIRST KIND

Tests of scaling of the first kind will be shown for the nuclei of this study in order of the nuclear mass A, then the mass of the probing beam, then by the increasing beam energy. Each case will cover the range of experimental momentum transfers for each hadron experiment. A figure summarizing the responses $\Phi(\psi)$ interpolated for $\psi = 0$ and $\psi = -0.8$ as the momentum transfer q increases will summarize the responses. Reference [33] carried out an analysis of electron spectra to test the convergence of the interpolated nonrelativistic responses on iron for large values of the four-momentum transfer Q^2. This work will use the three-momentum transfer q.

Figure 1 shows responses $\Phi(\psi)$ computed by the expressions in the Appendix for hadron data on a ^{6}Li sample, from negative pion [23] and proton [31] spectra. A Fermi momentum of $k_F = 165$ MeV/c [6] was used to compute the RFG curves. The pion spectra were taken with a broad acceptance spectrometer, with several overlapping magnetic field settings, and reported for fixed values of q. These data agree completely, until large energy losses are encountered at large
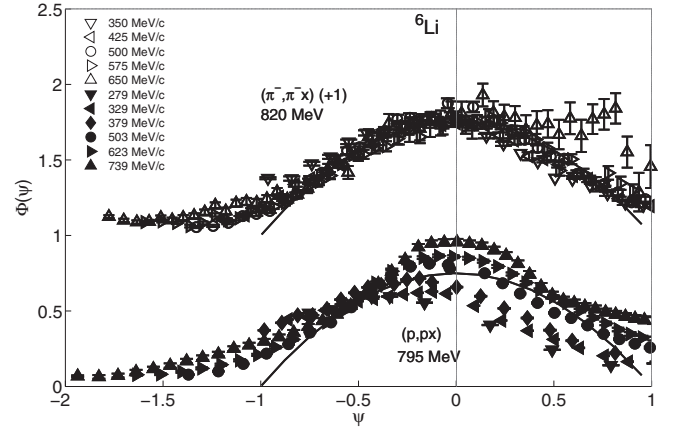

FIG. 1. Scaling of the first kind would imply that responses for a given beam on a given target are independent of momentum transfer. Two arrays of relativistic hadron beam NCX responses $\Phi(\psi)$ on ^{6}Li are shown as the three-momentum transfer q changes [23,31], compared to the RFG curve for $k_F = 165$ MeV/c [6], without Pauli blocking. Open points are for negative beams, and solid points are for positive beams.

momentum transfer, and match the RFG curve. This agreement demonstrates scaling of the first kind for 820 MeV π^- spectra from ^{6}Li. The 795 MeV proton data [31] increase steadily with increasing q, perhaps due to backgrounds from processes other than simple quasifree. The $q = 503$ MeV/c spectrum response for protons, meeting the conditions for quasifree scattering, lies near the RFG curve.

Clear quasifree peaks are found in the 500 MeV pion NCX responses for carbon [22] and are seen to be equal for both pion signs in Fig. 2. However, the 500 MeV data at three
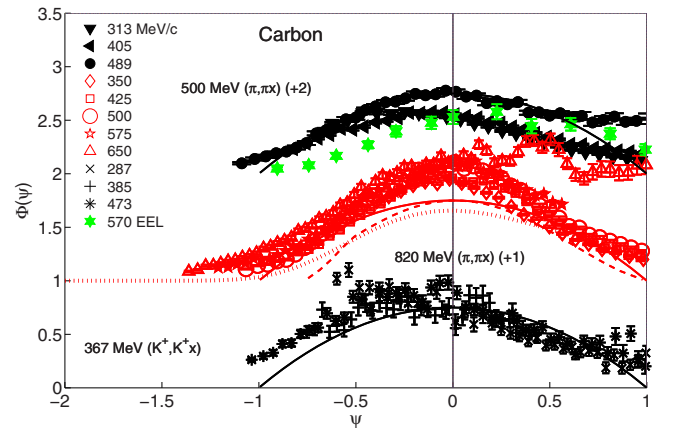

FIG. 2. Three data sets for meson NCX quasifree scattering on carbon are shown [22–24] in the $\Phi(\psi)$ format across a range of momentum transfers to test scaling of the first kind. Solid lines show the RFG expectation with $k_F = 228$ MeV/c for $q = 500$ MeV/c, and the dashed curve shows the effect of Pauli blocking at $q = 350$ MeV/c. The dotted curve shows the SuSAv2 nonspin isoscalar model response from the Appendix of Ref. [13]. With the 500 MeV pion spectra are also shown in green the $q = 570$ MeV/c carbon charge (EEL) responses from electron scattering [8]. The 820 MeV pion data are in red in the online figure.
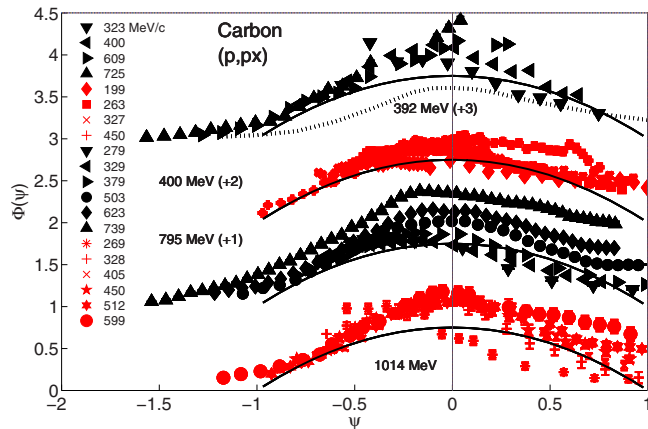
FIG. 3. Four data sets for proton NCX quasifree scattering on carbon are shown [25,28,31,32] in the $\Phi(\psi)$ format across a wide range of momentum transfers. Solid lines show the RFG expectation for $q = 500$ MeV/c. A dotted curve shows the "universal" curve for electron scattering [6]. The 400 MeV [28] and 1014 MeV [32] proton data are in red in the online figure.
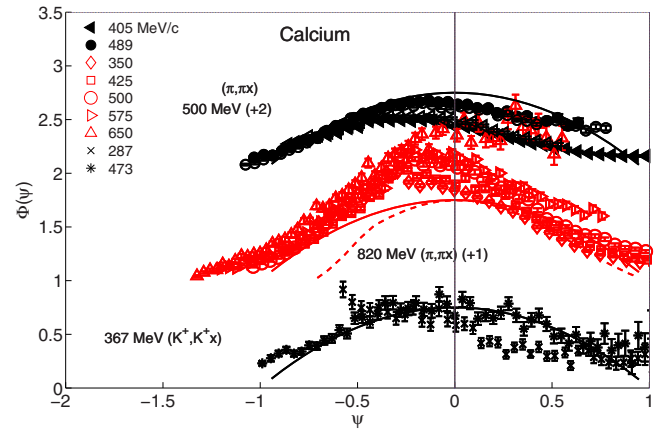

FIG. 4. Three data sets for meson NCX quasifree scattering on calcium are shown [22–24] in the $\Phi(\psi)$ format across a range of momentum transfers. Solid lines show the RFG expectation with $k_F = 241$ MeV/c for $q = 500$ MeV/c, and the dashed curve shows the effect of Pauli blocking at $q = 350$ MeV/c. The 820 MeV pion data are in red in the online figure.

momentum transfers do not show scaling of the first kind. For 820 MeV pions [23], the carbon responses show better scaling of the first kind, until pion production becomes important at large momentum transfer. Sparse data [24] for quasifree K^+ scattering scale quite well with increasing momentum transfer.

Computed responses in the SuSAv2 model were compared to electron quasifree data in Ref. [13], with fitted shapes in the Appendix of that work. A dotted curve for the "longitudinal" (nonspin) isoscalar response is compared to the 820 MeV π^- responses in Fig. 2. The hadron response may contain contributions from other spin/isospin channels to explain the observed difference.

Relativistic responses for four proton beam energies upon carbon are shown in Fig. 3. At 392 MeV [25] the responses fail to scale at large angles or momentum transfers, but converge well at negative ψ. At 400 MeV for smaller q [28], the carbon relativistic responses scale quite well. In contrast, the 795 MeV proton responses [31] fail to scale, due to a larger contribution from pion production at larger angles. At 1014 MeV [32], good scaling is found except at the smallest angle.

The shape of a universal relativistic response was shown in Ref. [6] and is reproduced as the dotted curve compared to the 392 MeV proton responses in Fig. 3. This curve is below the RFG shape and fails to match the proton data.

For calcium, the 500 MeV pion responses seen in Fig. 4 agree for the two pion signs [22] at two momentum transfers. At 820 MeV [23], better scaling is found except at large energy losses at the largest momentum transfer. As for carbon, the K^+ responses on calcium scale quite well [24]. Only the K^+ responses agree with the RFG curves for calcium.

The proton beam responses for calcium are seen in Fig. 5 at three beam energies. As for carbon, the 392 MeV responses rise rapidly for larger angles [26], but nearly scale at negative ψ. The 795 MeV proton responses on calcium [31] fail to scale, but the 1014 MeV data [32] are near the RFG curve.

Charge symmetry in cross sections is not expected for the zirconium ($A = 91$) sample, but the 500 MeV pion responses [22] agree in Fig. 6, since the elementary cross sections have been adjusted for the neutron excess. Scaling of the first kind is not noted except at very negative values of ψ. By 820 MeV, the pion responses scale more closely [23]. Proton responses at 392 MeV on niobium ($A = 93$) [27] are similar to those for the lighter nuclei, with a failure to scale except at very negative ψ, as seen in Fig. 6. This failure to scale is also noted at 795 MeV [31].

Pion responses for lead at 500 MeV [22] are shown in Fig. 7, but the responses are not found to be equal for the two beam signs. Much as for the lighter samples, the 820 MeV responses [23] nearly scale, as do the K^+ responses [24]. The relativistic responses $\Phi(\psi)$ for 392 MeV and 795 MeV protons fail to scale
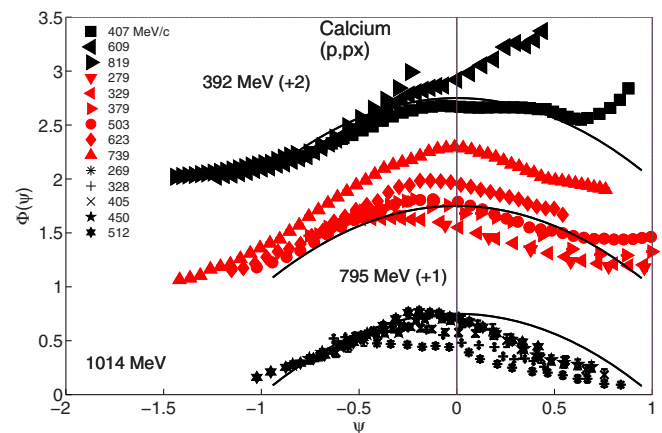

FIG. 5. Three data sets for proton NCX quasifree scattering on calcium are shown [26,31,32] in the $\Phi(\psi)$ format across a wide range of momentum transfers. Solid lines show the RFG expectation for $q = 500$ MeV/c. The 795 MeV proton data [31] are in red in the online figure.
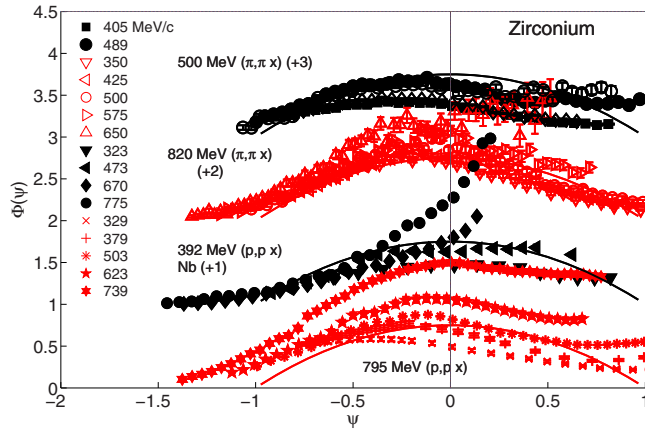
FIG. 6. Data arrays for both pion and proton NCX quasifree scattering on zirconium (or niobium) are shown [22,23,27,31] in the $\Phi(\psi)$ format across a wide range of momentum transfers to test scaling of the first kind. Solid lines show the RFG expectation for $q = 500$ MeV/c and $k_F = 245$ MeV/c [6]. The 820 MeV pion [23] and 795 MeV proton data [31] are in red in the online figure.

in much the same fashion as for lighter nuclei, as noted in Fig. 8. Responses computed in the coherent density fluctuation model (CDFM) are shown for gold at $q = 1000$ MeV/c [34,35].

These tests of scaling of the first kind for all the hadron quasifree data are summarized in Figs. 9 and 10, with interpolated responses at $\psi = 0$ and $\psi = -0.8$. All responses Φ at $\psi = 0$ rise with increasing momentum transfer, with best fit slopes listed in Table I. These straight-line fits are also shown with the $\psi = 0$ data in the figures. Interpolated responses at $\psi = -0.8$ are remarkably constant for all nuclei, with each consistent with an overall average of $\Phi(\psi = -0.8) = 0.361$. The RFG expectation at $\psi = -0.8$ is 0.27.
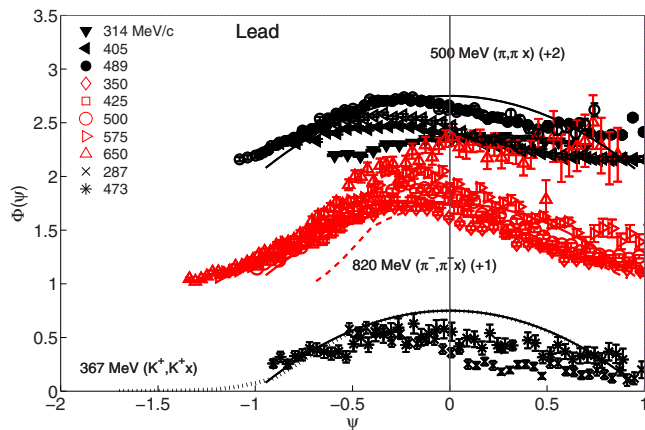

FIG. 7. Three data sets for meson NCX quasifree scattering on lead are shown [22–24] in the $\Phi(\psi)$ format across a range of momentum transfers. Solid lines show the RFG expectation with $k_F = 248$ MeV/c [6] for $q = 500$ MeV/c, and the dashed curve shows the effect of Pauli blocking at $q = 350$ MeV/c. A dotted curve shows the prediction of the coherent density fluctuation model (CDFM) for ^{197}Au at $q = 1000$ MeV/c [34]. The 820 MeV pion data are in red in the online figure.
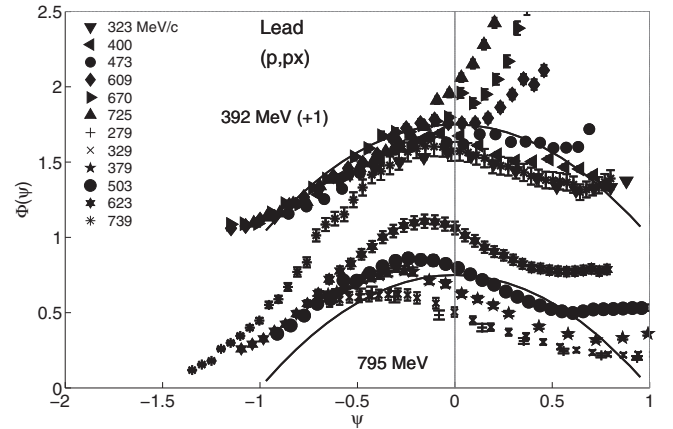

FIG. 8. Two proton data sets for NCX quasifree scattering on lead are shown [27,31]. Curves show the unblocked RFG expectation as in Fig. 7.

Thus, quasifree NCX hadron scattering responses agree as the momentum transfer increases with for scaling of the first kind at $\psi = -0.8$, and violate this scaling in a very simple manner at $\psi = 0$, with small slopes which increase with target mass A.

IV. SCALING OF THE SECOND KIND

Scaling of the second kind will be tested only for momentum transfers q near 500 MeV/c, without the blocking influence of the Pauli Principle and meeting the conditions for quasifree scattering.

Figure 11 includes the spectra for both pion signs at 500 MeV for a range of nuclear masses A [22]. These data cluster nicely for agreement with scaling of the second kind. For 820 MeV pions [23], this agreement is not found. Note the spike near the maximum responses for calcium; this sample had
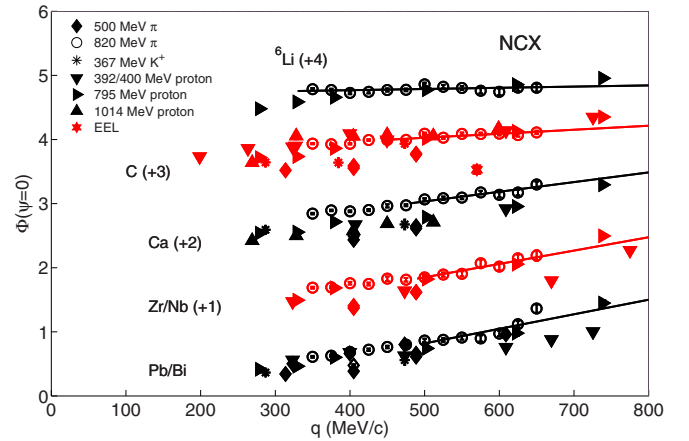

FIG. 9. Interpolated responses $\Phi(\psi)$ for NCX quasifree scattering on five nuclear samples are shown for $\psi = 0$, the expected maximum. The RFG expectation is $\Phi(\psi = 0) = 0.75$. Scaling of the first kind would imply that each response is independent of momentum transfer q. Linear fits are shown for the 820 MeV π^- responses with $q > 2k_F$, with parameters listed in Table I.
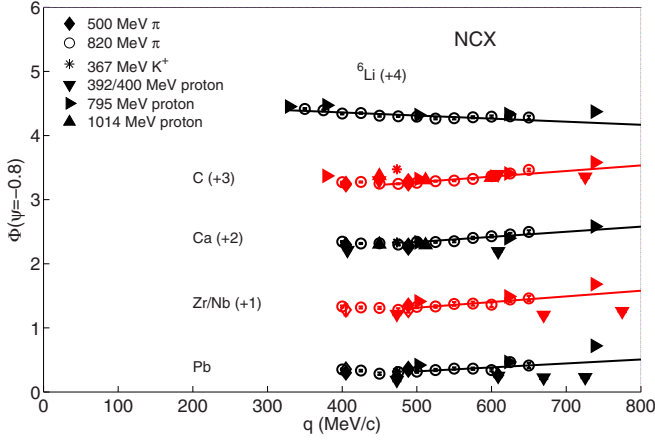
FIG. 10. As Fig. 9, but as interpolated at $\psi = -0.8$, where nuclear structure effects are more likely to be noted. The RFG expectation is $\Phi_{RFG}(y = -0.8) = 0.27$ and the CDFM prediction is 0.233 [34]. Scaling of the first kind would imply that the response for each nucleus is independent of the momentum transfer q. Linear fits for $q > 2k_F$ are shown as q increases, with parameters in Table I.

a significant hydrogen contaminant. This figure also shows the mass dependence for the K^+ beam [24]; within large scatter, these responses follow scaling of the second kind.

The 795 MeV proton experiment of Ref. [31] covered a wide range of samples, with responses seen in Fig. 12. Save for carbon, these responses scale with the nuclear mass A. This figure also compares the two masses for the 1014 MeV proton responses [31,32]; the data of this old experiment fail to follow scaling of the second kind over only two nuclei. A wider range of samples is spanned at 558 MeV [30], with general agreement with scaling at negative ψ.

Much as for scaling of the first kind, these results for scaling of the second kind are summarized in Fig. 13 by interpolations at $\psi = 0$ and $\psi = -0.8$ for q near 500 MeV/c. The terbium and tantalum proton points at 392 MeV also disagree in the tabulated spectra [27]. These interpolated responses $\Phi(\psi)$ are nicely constant with increasing mass, and agree with scaling of the second kind, with average responses $\Phi(\psi = -0.8) = 0.304(0.061)$ and $\Phi(\psi = 0) = 0.754(0.12)$. The relativistic Fermi gas (RFG) responses are very near $\Phi_{RFG}(y = -0.8) = 0.273$ and $\Phi_{RFG}(y = 0) = 0.75$.

Overall, at a momentum transfer not subject to Pauli blocking, the maxima $\Phi(\psi = 0)$ follow scaling of the second kind very closely. At lower energy losses, the simple RFG is not

TABLE I. Scaling of the first kind would exhibit responses $\Phi(\psi)$ that are independent of the momentum transfer q. Here are listed the slopes b of linear fits $\Phi(\psi) = a + bq$ for 820 MeV ($\pi^-, \pi^- x$) [23] with q at least $2k_F$, with q as the free momentum transfer in MeV/c.

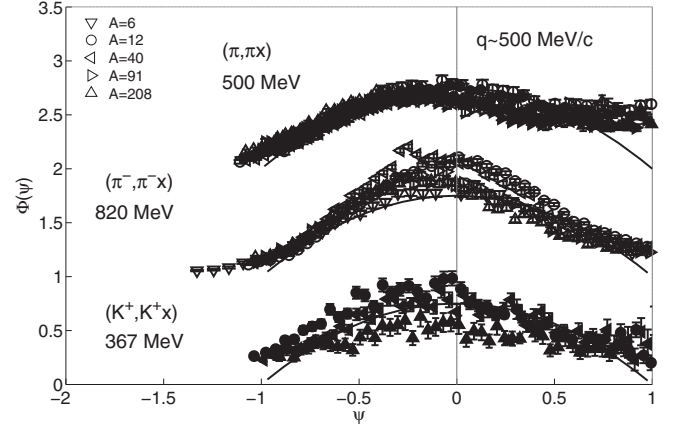|	$\psi = 0$	$\psi = -0.8$
^{6}Li	$1.86 \times 10^{-4}(0.94 \times 10^{-4})$	$-4.8 \times 10^{-4}(0.5 \times 10^{-4})$
Carbon	$6.26 \times 10^{-4}(0.97 \times 10^{-4})$	$8.7 \times 10^{-4}(0.6 \times 10^{-4})$
Calcium	$15.1 \times 10^{-4}(1.6 \times 10^{-4})$	$8.0 \times 10^{-4}(0.9 \times 10^{-4})$
Zirconium	$20.8 \times 10^{-4}(2.9 \times 10^{-4})$	$8.8 \times 10^{-4}(1.9 \times 10^{-4})$

FIG. 11. Scaling of the second kind would give responses $\Phi(\psi)$ the same for all target masses A. This is tested for three meson beams [22–24] for momentum transfers q near 500 MeV/c. The curves show the RFG for carbon, with $k_F = 228$ MeV/c. The calcium target for the 820 MeV experiment had a small hydrogen contamination [23], resulting in a sharp peak near $\psi = -0.3$.

adequate to account for the responses $\Phi(\psi = -0.8)$, which do follow scaling of the second kind.

V. SCALING OF THE THIRD KIND

Scaling of the third kind has been defined as observing quasifree responses that are the same for all elementary beams on a given nuclear sample at similar momentum transfers [16,17]; here, that momentum transfer is taken to be near 350 MeV/c or near 500 MeV/c. The two hadron beams [23,31] used for quasifree scattering on ^{6}Li show nearly identical responses $\Phi(\psi)$ in Fig. 14, for good agreement with this scaling of the third kind at 500 MeV/c. At $q = 350$ MeV/c, this figure also finds a close similarity between the pion data [23] and the proton data at 13 and 15 deg. ($q = 329$ and 379 MeV/c) [31].
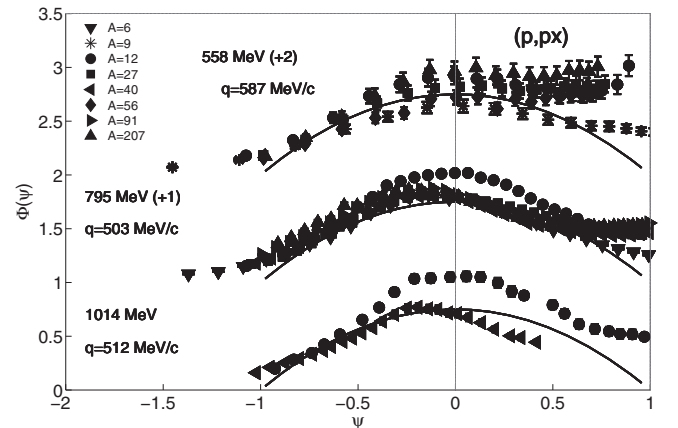

FIG. 12. NCX scaling responses for protons are shown for three beam energies at momentum transfers near 500 MeV/c on a range of nuclei [30–32]. The curves show the RFG expectation with $k_F = 228$ MeV/c, appropriate for carbon [6].
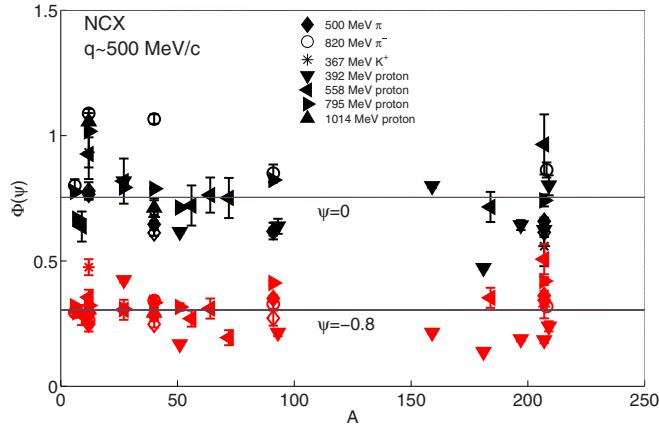
FIG. 13. NCX scaling responses interpolated for $\psi = 0$ and $\psi = -0.8$ are shown for several beams for a range of nuclear masses A. The averages are 0.754(0.12) and 0.304(0.061) at $\psi = 0$ and -0.8, respectively, in agreement with the RFG expectations 0.75 and 0.27. These data are for momentum transfers near 500 MeV/c. Scaling of the second kind would imply that each beam would exhibit no dependence upon the nuclear mass A. Citations for the data can be found in the text. Interpolated responses at $\psi = -0.8$ are in red in the online figure.

Responses $\Phi(\psi)$ for carbon are shown at both q near 350 and near 500 MeV/c in Fig. 15. At q near 350 MeV/c, not fully matching the quasifree conditions, the hadron responses nearly agree, but are stronger than expected by the Pauli-blocked RFG curve. Some of the hadron responses near $q = 500$ MeV/c, but not all, match the RFG curve.

Similar responses for calcium for five hadron beams are seen in Fig. 16, with an apparent difference between proton and meson results. For zirconium/niobium responses, two patterns each agree in Fig. 16. For five hadron beams on lead or bismuth
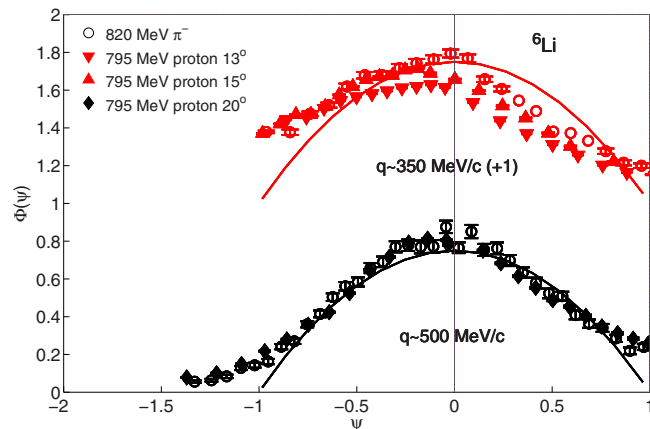

FIG. 14. Scaling of the third kind [16,17] would imply that for a given nucleus at the same momentum transfer, all hadron beams would exhibit the same responses. Relativistic responses $\Phi(\psi)$ are compared for two momentum transfers for ^{6}Li, with data from Refs. [23,31]. For $q = 350$ MeV/c, the proton data are shown at both 13 deg. ($q = 329$ MeV/c) and 15 deg. ($q = 379$ MeV/c). Curves show the unblocked expectations of the RFG.
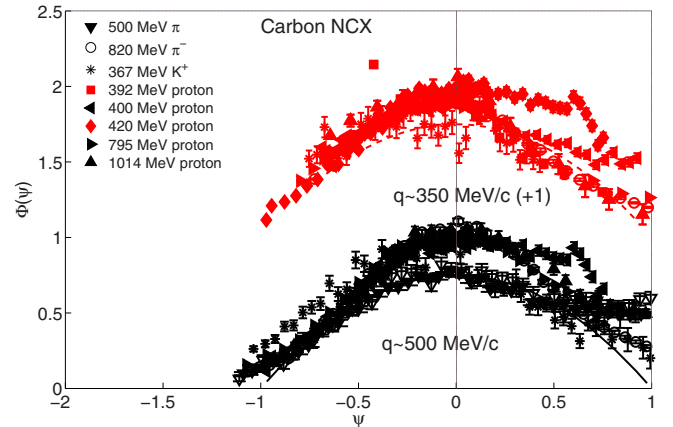

FIG. 15. NCX scaling responses $\Phi(\psi)$ are shown for a carbon sample for several beams, with q near 350 and 500 MeV/c. The curves show the carbon RFG expectation, including Pauli blocking at $q = 350$ MeV/c. Citations to the data can be found in the text.

with q near 500 MeV/c, Fig. 16 finds good agreement with scaling of the third kind, save at the lowest beam energy.

It has been suggested that K^+ mesons encounter "swollen nucleons" within nuclei [36,37]. The data shown for carbon, calcium, and lead in Figs. 15 and 16 follow the same analysis as for other hadron beams, with A_{eff} computed for 70% of the free-space total cross sections and free off-shell beam nucleon differential cross sections. The computed responses do not differ from those of other hadrons.

These interpolated responses are shown in Fig. 17 plotted against the in-medium (70% of free space) total cross sections SGT [38,39]. The hadronic data have been fit to a linear dependence, as shown, with parameters listed in Table II. A carbon datum from electron scattering at $q = 570$ MeV/c is also shown [8], as are (e, ex) responses at $q = 460$ MeV/c from Ref. [2].

The nuclear density dependence for scaling of the third kind is shown for three nuclei in Fig. 18 at both $\psi = 0$ and
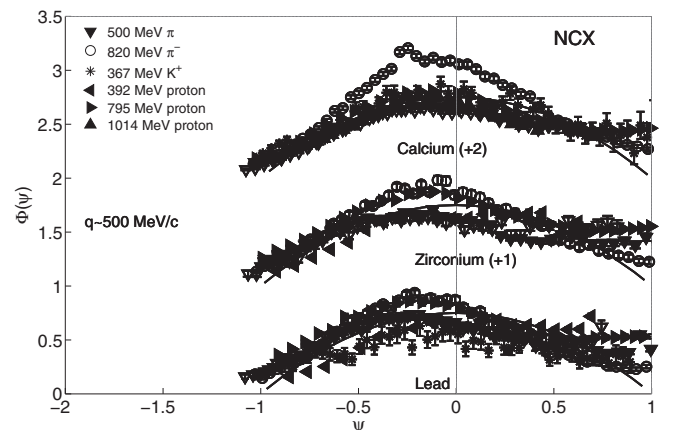

FIG. 16. To test scaling of the third kind for heavier nuclei, NCX scaling responses $\Phi(\psi)$ are shown for three nuclei, with q near 500 MeV/c. Citations are found in the text. Curves show the RFG expectations for $q = 500$ MeV/c.
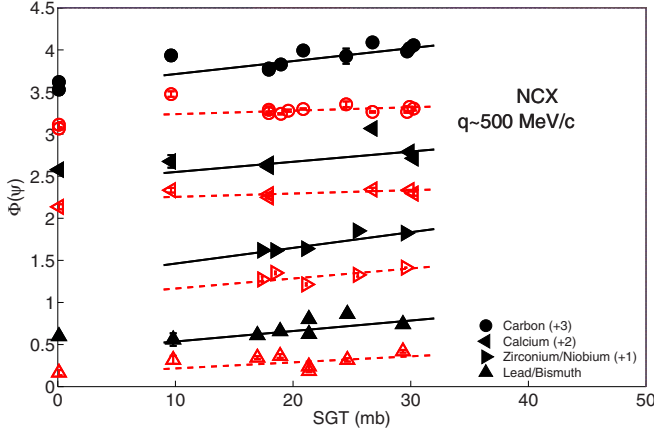
FIG. 17. Interpolated responses for several beams for four nuclei are shown as the in-medium beam-nucleon total cross section SGT changes; results for $\psi = 0$ are in solid black, and the lower open points for $\psi = -0.8$ are in red in the online figures. Momentum transfers q are near 500 MeV/c. The fitted lines use the parameters found in Table II. Carbon points for electron scattering are at $q = 570$ MeV/c [8], while three points for both $\psi = 0$ and $\psi = -0.8$ are determined at $q = 460$ MeV/c [2].
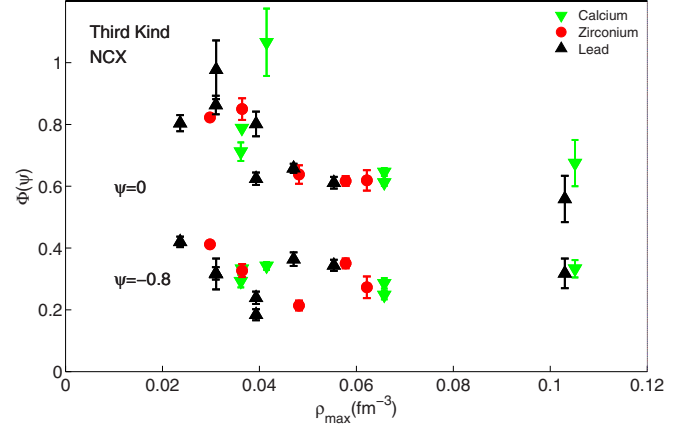

FIG. 18. The computed effective numbers of nucleons A_{eff} for three nuclei and several hadron beams were used to compute the maximum nuclear density ρ_{max} reached at R_{min} in the Glauber method with 70% of free-space SGT. Interpolated responses for $\psi = -0.8$ and $\psi = 0$ are plotted for several hadron beams as far as those densities. At $\psi = -0.8$ the RFG expectation is $\Phi(\psi = -0.8) = 0.27$, and $\Phi(\psi = 0) = 0.75$. The K^+ beam reaches the greatest densities, the proton beams the least density. The electron figures of Ref. [2] at $q = 460$ MeV/c at central densities of 0.171 and 0.1637 fm^{-3} give responses of 0.577(0.03) and 0.598(0.03) at $\psi = 0$ for calcium and lead, and 0.136(0.03) and 0.166(0.03) at $\psi = -0.8$. These lie on smooth continuations of the hadron data.

$\psi = -0.8$. Here, the maximum nuclear density reached by each beam in each nucleus is used as the measure. This density is that at a radius outside of which the nuclear volume integrates to equal A_{eff}. The Appendix describes the method. At $\psi = -0.8$, these responses are constant to a nuclear density of 0.1 nucleons/fm^3 for all targets, while at $\psi = 0$, the responses indicate an increase at low densities.

VI. CONCLUSIONS

A wide range of hadron spectra that meet the formal conditions for incoherent quasifree scattering have been transformed to relativistic single-nucleon responses as familiar from many electron scattering analyses. The methods used for the more complex strong interactions are summarized in the Appendix. The two types of scaling identified for electron scattering and the third kind defined for hadron and electroweak spectra have been tested, and the scaling conclusions will be summarized here.

Scaling of the first kind would be recognized by responses for scattering on a given nucleus by a given beam that are

independent of the momentum transfer q. Such scaling has been found for electrons scattered by nucleon charges, with a universal curve found to represent such data [4]. The hadron beam relativistic responses $\Phi(\psi)$ have been shown for pion, K^+, and proton beams in Figs. 1–9 and summarized in Fig. 10. Since the Fermi gas model for bound nucleons does obey scaling of the first kind, the appropriate RFG responses have been compared to the hadron data.

Table I summarizes a test of scaling of the first kind, with fits for five nuclei of the responses at $\psi = 0$ and $\psi = -0.8$ as the free elastic momentum transfer q increases for 820 MeV (π^-, π^-x) data [23]. Only responses with $q > 2k_F$ were fit, and only the slopes are listed; scaling of the first kind would find these slopes to be zero. Slopes are slightly positive and increase slowly for heavier nuclei. Scaling of the first kind is not found, but the data exhibit a consistent pattern.

TABLE II. Scaling of the third kind would be noted if responses $\Phi(\psi)$ on a given nuclear sample at the same momentum transfer near 500 MeV/c are the same for all hadron beams. Parameters for linear fits at interpolated values of ψ are shown for changing values of SGT as $\Phi(\psi) = a + b$ SGT. This variable SGT is computed as 70% of the neutron/proton average of free-space hadron-nucleon total cross sections in mb [38,39].

	$\psi = 0$		$\psi = -0.8$	
	a	b (mb^{-1})	a	b (mb^{-1})
Carbon	0.559 (0.029)	0.0154 (0.0010)	0.195 (0.014)	0.0041 (0.0005)
Calcium	0.427(0.021)	0.0122 (0.0007)	0.215(0.023)	0.0040 (0.0008)
Zr/Nb	0.275 (0.039)	0.0187 (0.0015)	0.046 (0.036)	0.0119 (0.0014)
Pb/Bi	0.411 (0.045)	0.0124 (0.0021)	0.144 (0.036)	0.0072 (0.0016)

Scaling of the second kind would be recognized by responses that are the same for all nuclei for a given beam at similar momentum transfers. Such scaling has been noted for electron "longitudinal" scattering from nucleon charge but is violated for transverse scattering, especially at large energy losses, including pion production, for instance, as noted in Ref. [2]. The hadron relativistic responses $\Phi(\psi)$ for pions, K^+, and protons have been shown in Figs. 11 and 12,

Fits to interpolated responses at $\psi = 0$ and -0.8 as the nuclear mass A changes have been made using $\Phi(\psi) = a + b\,A$. For $\psi = 0$, $a = 0.8535(0.0017)$, and $b = -0.00165(0.00003)$. For $\psi = -0.8$, $a = 0.314(0.015)$, and $b = -0.00065(0.00002)$. At both values of ψ, the slopes are small and negative. Scaling of the second kind is closely followed. This is a confirmation mainly of the Glauber method used to compute A_{eff}. If scaling of the second kind is assumed, the average values of the responses are 0.754(0.117) at $\psi = 0$ and 0.303(0.061) at $\psi = -0.8$.

Superscaling has been defined for those responses that follow both scaling of the first and second kinds [3,12,14,15]. The present results find this nearly to be valid for hadrons. Electron scattering with a spin transfer of zero does follow Superscaling [2], but when a unit of spin is transferred, this superscaling is lost [2].

A scaling of the third kind for quasifree spectra has been defined [16,17], with relativistic responses for three hadrons and five nuclei shown in Figs. 15 and 16, summarized in Fig. 17. Within the Glauber method, these responses are shown as a function of the maximum nuclear density reached in Fig. 18, with differences between the responses at $\psi = 0$ and $\psi = -0.8$.

Table II lists parameters for fits to test this scaling of the third kind, with the total average (neutron/proton) cross sections SGT as the variable, using 70% of the free-space total cross sections SGT in mb [38,39] in $\Phi(\psi) = a + b$ SGT. Only hadron responses with q near 500 MeV/c were used for these fits. Although the slopes are not zero, as expected for scaling of the third kind, they are small. This may be due to the fact that NCX spectra are dominated by isoscalar, nonspin interactions [38]. The range of hadron beams allows a study of the nuclear density reached by K^+, pions, and protons, and seem to indicate agreement with the electron scattering responses in Fig. 17. The hadron relativistic single-nucleon responses for three nuclei show consistent trends in Fig. 18.

If the relativistic single-particle responses for electrons and hadrons follow all three types of scaling, one can only call this Hyperscaling. A wide range of hadron NCX responses find this nearly to be valid.

It is a weakness of the methods used to create the hadron responses that the restriction to the nuclear surface is noted only through the Glauber approximation to count single collisions. A more effective way to see actual nuclear effects in that surface would be to compute responses for nucleons in the surface, for instance by RPA methods. This was shown to match the data for two samples of early hadron quasifree spectra in the work of Alberico *et al.* in Ref. [40]. It would surely be of value to extend such work to the much richer array of hadron data available now, both NCX and purely isovector single charge

exchange (SCX) spectra. Methods similar to the present have examined many SCX spectra for scaling properties [41].

It is an interesting idea to suggest that failures to scale for hadron quasifree spectra may be due to differences between the nuclear single-nucleon responses and those in free space. Future publications will explore a selection procedure to find where data indeed represent these quasifree scattering events that represent single-nucleon responses, similar to the work with electron scattering data [42–44].

APPENDIX

In this Appendix the expressions for the quasifree scaling relations used in this work will be defined, and the usage of terms in these expressions will be given. The definitions and terminology will be much the same as used for analyses of quasifree electron scattering [2,45,46].

The scaling variable is taken to be ψ, much as defined in Ref. [2]. This variable is the relativistic analog of the variable y [45], which is the least momentum of the single bound moving nucleon that can scatter a beam particle to a given energy loss ΔE and momentum transfer q. This ψ is expressed as a fraction of the Fermi momentum k_F, as tabulated in Ref. [6].

The momentum transfer is that to the beam hadron, corrected to be the effective momentum transfer as the charged hadron strikes the charged nucleus Z with mass A

$$q_{\text{eff}} = q(1 +/- 4Ze^2/3\text{T}r_0 A^{1/3}). \tag{A1}$$

Here, T is the kinetic energy of the beam hadron, with the plus sign for a negative beam, and $r_0 = 1.2$ fm. Hereafter, this q_{eff} is referred to as simply q. Plots versus q cite the free beam-nucleon elastic momentum transfer.

The energy transfer ω to the single bound nucleon includes the least recoil energy of the other $A - 1$ nucleons, which is

$$\text{Recoil} = y^2/2M(A - 1), \tag{A2}$$

with y the nonrelativistic momentum of the bound nucleon (equal to that of the rest of the $A - 1$ nucleons),

$$y = [\omega(\omega + 2M)]^{1/2} - q. \tag{A3}$$

In this work, M is the free nucleon mass. Recent electron scattering analyses have found a best fit to an effective mass of 0.8M [42–44], but hadrons interacting in the nuclear surface seem to indicate the free mass.

A separation energy for the bound nucleon is included in the energy loss ω, from Ref. [6]. For SCX, the mass difference Q between the incoming and outgoing hadrons is included in SE. Also, for SCX, a Coulomb energy CE $= Ze^2/r_0 A^{1/3}$ is added or subtracted to SE to form ω. For pion SCX with both signs on bismuth, this Coulomb energy for each beam sign is 16.8 MeV. Then,

$$\omega = \Delta E - \text{SE} = \Delta E - Q - \text{CE-separation energy-Recoil.} \tag{A4}$$

My sign convention is that positive terms remove kinetic energy from the beam. Overall, dropping terms with $\omega \ll 2M$ simplifies this energy transfer to the single struck nucleon

to

$$\omega = \{2q^2 + A[2M(A-1)(\Delta E - \mathrm{SE}) - q^2]$$
$$+ 2q[q^2 + 2MA(A-1)(\Delta E - \mathrm{SE}) - Aq^2]^{1/2}\}/2MA^2.$$
(A5)

Then,

$$\psi = (\lambda - \tau)/\xi_F^{1/2}\{(1+\lambda)\tau + k[\tau(\tau+1)]^{1/2}\}, \quad (A6)$$

with $\xi_F = (1 + \eta_F^2)^{1/2} - 1$ as the dimensionless Fermi kinetic energy, $\eta_F = k_F/M$, $\tau = \kappa^2 - \lambda^2$, $\lambda = \omega/2M$ and $\kappa = q/2M$ [2,8,14]. The free nucleon mass is M. When the SE is included in ω Refs. [2,13] call this variable ψ'.

The relativistic response is formed from the measured doubly-differential cross section data as

$$\Phi(\psi) = d^2\sigma/d\Delta E d\Omega \quad d\Delta E/d\psi/d\sigma/d\Omega \, A_{\mathrm{eff}}. \quad (A7)$$

The transformation from lab energy loss ΔE to the beam hadron to the variable ψ is evaluated numerically. The optimum frame method [47] is used to evaluate the singly-differential cross sections $d\sigma/d\Omega$ across the energy loss data of the NCX spectrum, suitably averaged over nuclear protons and neutrons. This method provides the beam energy and scattering angle for the same momentum transfer as the experiment for a moving bound nucleon; these optimum frame beam energies change slowly for $\psi < 0$. These singly-differential cross sections are then evaluated using the fits and compilation of SAID [38]. Beam energies are higher and scattering angles are lower for negative ψ. The case of $\psi = 0$ would correspond to a collision with a bound nucleon at rest. For large positive ψ these off-shell cross sections can vary rapidly, and become unreliable, which limits the range of this scaling system. For pion beams, where free scattering encounters resonances not observed in pion reactions with nuclei, the off-shell cross sections in the denominator are averaged for the beam energy and ± 18 MeV.

The large cross sections for hadron beams upon nucleons imply that fewer than all A nucleons in a nucleus may be struck once-and-only-once. The counting of such nucleons is accomplished in the Glauber model [48], as used in Ref. [49]. In-medium pion-nucleon and proton-nucleon total cross sections SGT are evaluated at 70% of the free-space values to account for the anticipated decrease due to Pauli blocking [50–53]. This choice led to the best agreement of scaling relations for hadrons on nuclei [54]. For K^+-nucleon scattering, 70% of free space cross sections are also used [39], in spite of some beliefs that this hadron encounters "swollen nucleons" [36,37]. Matter, not charge, distributions of nuclei $\rho(r)$ were taken from Ref. [55], with the same geometrical parameters for neutrons and protons.

The expression used for the effective number of nucleons A_{eff} struck once-and-only-once [48,49] is

$$A_{\mathrm{eff}} = \int T(b)e^{-\mathrm{SGT}T(b)}2\pi b \, db, \quad (A8)$$

with the profile function

$$T(b) = \int \rho(r)dz \quad (A9)$$

for an impact parameter b, proceeding straight through the target nucleus along z, with SGT as 70% of the free-space average hadron-nucleon total cross section [38,39]. It is worth noting that nucleon final state interactions included in electron scattering analyses also use a similar Glauber method [8].

To estimate the radius and density reached by hadron beams, the computed A_{eff} is taken to be the volume integral of the nuclear density beyond some R_{min}. The nuclear density at R_{min} is taken to be the maximum nuclear density sensed by each hadron beam.

The resulting responses $\Phi(\psi)$ are compared in the figures to the expectation for a relativistic Fermi gas (RFG) of bound nucleons [1–4], which includes a small term of the variable ψ to the fourth power:

$$\Phi(\psi)_{\mathrm{RFG}} = 0.75(1-\psi^2)\Theta(1-\psi^2)\{\eta_F^2 + \psi^2[2 + \eta_F^2$$
$$- 2(1 + \eta_F^2)^{1/2}]\}/\eta_F^2. \quad (A10)$$

This RFG response must be modified for momentum transfers q less than twice k_F by Pauli blocking, in which the momentum states of the bound nucleons are filled, and recoil into those states is forbidden. This blocking term depends upon both the energy loss ω and momentum transfer q. The integral of this blocking decreases the singly-differential cross section by a factor [21]

$$\mathrm{PBFI} = 3q/4k_F - q^3/16k_F^3. \quad (A11)$$

This factor has been shown to match the integrated cross sections for quasifree hadron scattering to form sum rules [20].

The shape of the doubly differential RFG across the energy loss spectrum is also blocked by factors given by the Lindhard function [56]:

$$\mathrm{PBF} = 2M\omega/k_F^2 \quad \text{for } \omega < qk_F/M - q^2/2M, \quad (A12)$$

$$\mathrm{PBF} = 1-z^2 \quad \text{for } \omega > qk_F/M - q^2/2M, \text{ but } \omega < qk_F/M$$
$$+ q^2/2M. \quad (A13)$$

Here, $z = M\omega/qk_F - q/2k_F$. The PBF is zero beyond the bounds of $\omega = qk_F/M +/- q^2/2M$ or for $|\psi| > 1$, but PBF = 1 for $q > 2k_F$ for $|\psi| < 1$. The Pauli-blocked relativistic Fermi gas expectation is called PBRFG in the figures.

---

[1] W. M. Alberico, A. Molinari, T. W. Donnelly, E. L. Kronenberg, and J. W. Van Orden, Phys. Rev. C **38**, 1801 (1988).

[2] T. W. Donnelly and I. Sick, Phys. Rev. C **60**, 065502 (1999).

[3] A. N. Antonov, M. K. Gaidarov, D. N. Kadrev, M. V. Ivanov, E. M. de Guerra, and J. M. Udias, Phys. Rev. C **69**, 044321 (2004).

[4] J. E. Amaro, M. B. Barbaro, J. A. Caballero, T. W. Donnelly, A. Molinari, and I. Sick, Phys. Rev. C **71**, 015501 (2005).

[5] M. L. Goldberger and K. M. Watson, *Collision Theory* (Wiley, New York, 1964).

[6] C. Maieron, T. W. Donnelly, and I. Sick, Phys. Rev. C **65**, 025502 (2002).

[7] E. J. Moniz, I. Sick, R. R. Whitney, J. R. Firenec, R. D. Kephart, and W. P. Trower, Phys. Rev. Lett. **26**, 445 (1971).

[8] J. E. Sobczyk, N. Rocco, A. Lovato, and J. Nieves, Phys. Rev. C **97**, 035506 (2018).

[9] K. S. Kim and L. E. Wright, Phys. Rev. C **68**, 027601 (2003).

[10] I. C. Cloet, W. Bentz, and A. W. Thomas, Phys. Rev. Lett. **116**, 032701 (2016).

[11] R. J. Peterson, Phys. Rev. C **85**, 064616 (2012).

[12] A. N. Antonov, M. V. Ivanov, J. A. Caballero, M. B. Barbaro, J. M. Udias, E. Moya de Guerra, and T. W. Donnelly, Phys. Rev. C **83**, 045504 (2011).

[13] R. González-Jiménez, G. D. Megias, M. B. Barbaro, J. A. Caballero, and T. W. Donnelly, Phys. Rev. C **90**, 035501 (2014).

[14] A. N. Antonov, M. K. Gaidarov, M.V. Ivanov, D. N. Kadrev, E. Moya de Guerra, P. Sarriguren, and J. M. Udias, Phys. Rev. C **71**, 014317 (2005).

[15] A. N. Antonov, M. V. Ivanov, M. K. Gaidarov, and E. M. de Guerra, Phys. Rev. C **75**, 034319 (2007).

[16] R. J. Peterson, Nucl. Phys. A **769**, 95 (2006).

[17] J. A. Caballero, J. E. Amaro, M. S. Barbaro, R. W. Donnelly, and J. M. Udias, Phys. Lett. B **653**, 366 (2007).

[18] G. A. Miller, Nucl. Phys. B **112**, 223 (2002).

[19] J. E. Sobczyk, Phys. Rev. C **96**, 045501 (2017).

[20] R. J. Peterson, Phys. Rev. C **97**, 024609 (2018).

[21] J. E. Wise, M. R. Braunstein, S. Høibråten, M. D. Kohler, B. J. Kriss, J. Ouyang, R. J. Peterson, J. A. McGill, C. L. Morris, S. J. Seestrom, R. M. Whitton, J. D. Zumbro, C. M. Edwards, and A. L. Williams, Phys. Rev. C **48**, 1840 (1993).

[22] J. D. Zumbro, C. L. Morris, J. A. McGill, S. J. Seestrom, R. M. Whitton, C. M. Edwards, A. L. Williams, M. R. Braunstein, M. D. Kohler, B. J. Kriss, S. Høibråten, R. J. Peterson, J. Ouyang, J. E. Wise, and W. R. Gibbs, Phys. Rev. Lett. **71**, 1796 (1993); J. D. Zumbro *et al.*, private communication (2010).

[23] Y. Fujii *et al.*, Phys. Rev. C **64**, 034608 (2001); Ph.D. thesis, Tohoku University (1998).

[24] C. M. Kormanyos, R. J. Peterson, J. R. Shepard, J. E. Wise, S. Bart, R. E. Chrien, L. Lee, B. L. Clausen, J. Piekarewicz, M. B. Barakat, E. V. Hungerford, R. A. Michael, K. H. Hicks, and T. Kishimoto, Phys. Rev. C **51**, 669 (1995); Ph.D. thesis, University of Colorado (1994).

[25] T. Kin, F. Saiho, S. Hohara, K. Ikeda, K. Ichikawa, Y. Yamashita, M. Imamura, G. Wakabayashi, N. Ikeda, Y. Uozumi, M. Matoba, M. Nakano, and N. Koori, Phys. Rev. C **72**, 014606 (2005).

[26] A. A. Cowley, G. F. Steyn, Y. Watanabe, T. Noro, K. Tamura, M. Kawabata, K. Hatanaka, H. Sakaguchi, H. Takeda, and M. Itoh, Phys. Rev. C **62**, 064604 (2000).

[27] H. Iwamoto, M. Imamura, Y. Koba, Y. Fukui, G. Wakabayashi, Y. Uozumi, T. Kin, Y. Iwamoto, S. Hohara, and M. Nakano, Phys. Rev. C **82**, 034604 (2010).

[28] H. Otsu, Ph.D. thesis, University of Tokyo (1995).

[29] C. Chan *et al.*, Nucl. Phys. A **510**, 713 (1990).

[30] S. M. Beck and C. A. Powell, NASA Technical Note D-8119, Washington, DC (1976).

[31] R. E. Chrien, T. J. Krieger, R. J. Sutter, M. May, H. Palevsky, R. L. Stearns, T. Kozlowski, and T. Bauer, Phys. Rev. C **21**, 1014 (1980).

[32] D. M. Corley *et al.*, Nucl. Phys. A **184**, 437 (1972).

[33] D. B. Day, J. S. McCarthy, Z. E. Meziani, R. Minehart, R. Sealock, S. T. Thornton, J. Jourdan, I. Sick, B. W. Filippone, R. D. McKeown, R. G. Milner, D. H. Potterveld, and Z. Szalata, Phys. Rev. Lett. **59**, 427 (1987).

[34] A. N. Antonov, M. V. Ivanov, M. K. Gaidarov, E. Moya de Guerra, P. Sarriguren, and J. M. Udias, Phys. Rev. C **73**, 047302 (2006).

[35] A. N. Antonov, M. V. Ivanov, M. B. Barbaro, J. A. Caballero, and E. M. de Guerra, Phys. Rev. C **79**, 044602 (2009).

[36] G. E. Brown, C. B. Dover, P. B. Siegel, and W. Weise, Phys. Rev. Lett. **60**, 2723 (1988).

[37] C. M. Kormanyos and R. J. Peterson, Nucl. Phys. A **585**, 113 (1995).

[38] SAID http://gwdac.physics.gwu.edu

[39] C. Patrignani *et al.* (Particle Data Group), Chin. Phys. C **40**, 100001 (2016).

[40] W. M. Alberico, A. De Pace, M. Ericson, M. B. Johnson, and A. Molinari, Phys. Rev. C **38**, 109 (1988).

[41] R. J. Peterson, Nucl. Phys. A **769**, 115 (2006); **803**, 46 (2008); **920**, 20 (2013).

[42] J. E. Amaro, E. Ruiz Arriola, and I. Ruiz Simo, Phys. Rev. C **92**, 054607 (2015).

[43] V. L. Martinez-Consentino, I. Ruiz Simo, J. E. Amaro, and E. Ruiz Arriola, Phys. Rev. C **96**, 064612 (2017).

[44] J. E. Amaro, E. Ruiz Arriola, and I. Ruiz Simo, Phys. Rev. D **95**, 076009 (2017).

[45] D. B. Day, J. S. McCarthy, T. W. Donnelly, and I. Sick, Ann. Rev. Nucl. Part. Sci. **40**, 357 (1990).

[46] O. Benhar, D. Day, and I. Sick, Rev. Mod. Phys. **80**, 189 (2008).

[47] S. A. Gurvitz, Phys. Rev. C **33**, 422 (1986).

[48] R. J. Glauber, in *Lectures in Theoretical Physics*, edited by W. J. Brittin and L. G. Dunham (Wiley, New York, 1959), Vol. 1, p. 315.

[49] J. Ouyang, S. Hoibraten, and R. J. Peterson, Phys. Rev. C **47** 2809 (1993).

[50] R. D. Smith and M. Bozoian, Phys. Rev. C **39**, 1751 (1989).

[51] L. Ray, Phys. Rev. C **41** 2816 (1990).

[52] J. J. Kelly, Phys. Rev. C **54**, 2547 (1996).

[53] C. Fuchs, A. Faessler, and M. El-Shabshiry, Phys. Rev. C **64**, 024003 (2001).

[54] R. J. Peterson, Nucl. Phys. A **740**, 119 (2004).

[55] J. D. Patterson and R. J. Peterson, Nucl. Phys. A **717**, 235 (2003).

[56] T. Ericson and W. Weise, *Pions and Nuclei* (Clarendon Press, Oxford,1988).